

# A sun sensor implemented with an asynchronous luminance vision sensor

J. A. Leñero-Bardallo  
and J. M. Guerrero-Rodríguez  
Escuela Superior Ingeniería  
Universidad de Cádiz  
Avda. Universidad de Cádiz 10  
Puerto Real 11519, Spain  
Emails: {juanantonio.lenero,  
josem.guerrero}@uca.es

L. Farian  
Nanoelectronics Group  
Department of Informatics  
University of Oslo  
Blindern 1072  
Oslo, Norway  
Email: lukaszf@ifi.uio.no

R. Carmona-Galán and  
Á. Rodríguez-Vázquez  
IMSE-CNM,  
CSIC-Universidad de Sevilla  
Av/ Américo Vespucio s/n,  
41092, Seville, Spain  
Emails: {rcarmona,  
angel}@imse-cnm.csic.es

**Abstract**—A sun sensor implemented with a spiking pixel matrix is reported. It is the very first one based on an asynchronous event-based pixel array. A paradigm associated to classic digital sun sensors is solved with this approach. Only pixels illuminated by the sun light are readout. Hence, the output data flow is quite reduced. The computational load to resolve the sun position is quite low, comparing to prior sensors. Sensor's latency is in the order of milliseconds. The advantages over implementations with APS pixels are more reduced data flow, less latency, and higher dynamic range.

**Keywords:** Sun sensors, AER, Attitude determination, Event-based vision sensors, Space probes.

## I. INTRODUCTION

Sun sensors are devices on demand to determine the sun position. They have multiple applications. For instance, solar power plants need to know precisely it to adjust accordingly the position of solar cells or heliostats. Sounding rockets and spacecrafts use the sun position to navigate. In this case, fast operation and low power consumption are mandatory. There are two main kinds of sun sensors: analog and digital. Analog sun sensors [1], [2] usually use two different photoactive regions to sense two different photocurrent values. The ratio between them, depends on the sun inclination. They have fast operation and low output data flow. Unfortunately, they are sensitive to mismatch and distractors. Digital sun sensors [3], [4] are built with an image sensor with APS pixels. The entire pixel matrix is readout. Then, the output data is processed to compute the sun position. Digital sun sensors overcome some of the limitations of analog ones, but still they have inherent drawbacks. Although there is a very low number of illuminated and meaningful pixels, the entire pixel matrix has to be readout and processed. This limits the operation speed and increases the computational time. Also, the choice of the integration time complicates the sensor operation. The dynamic range is usually limited to 60-70dB. To amend some of the aforementioned limitations, some authors have presented approaches based on the determination of a Region of Interest (ROI) which the illuminated pixels, that are readout and processed. However, to determine the ROI requires to readout pixels that are dark

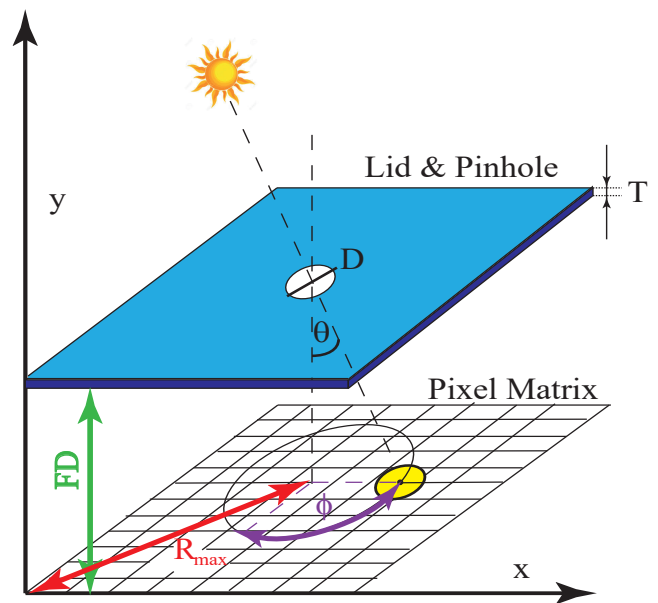


Fig. 1. System implementation sketch. There is a pixel array covered by an opaque lid with a pinhole in its center. Only a reduced number of pixels are illuminated through the pinhole by the sun light projection. Depending on the sun inclination with the sensor's vertical axis, different pixels will be illuminated.

and not meaningful. In this article, a new approach based on an asynchronous event-based pixel vision sensor is presented. Only illuminated pixels can send information out of the sensor. There is no need of choosing an integration time to operate. Reading out only one single pixel output, it is possible to resolve the sun position. Furthermore, sensor's dynamic range is higher than in conventional digital sensors with APS pixels.

## II. SYSTEM IMPLEMENTATION

Fig. 1 depicts how the optics is arranged. The chip is covered with an opaque lid with a pinhole lens [3], [4]. The sun light illuminates different groups of pixels, depending on the sun position. It is possible to express the latitude,  $\theta$ , and

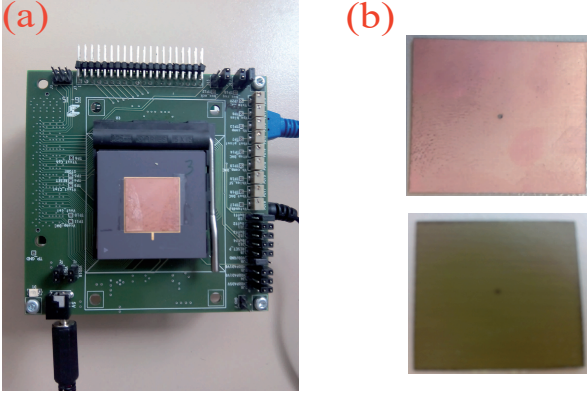


Fig. 2. (a) Sensor's front view. Dimensions are 9.5cm×9.5cm. (b) Detail of the lid with a pinhole. The side that faces the sun is metallic to reflect the sun radiation. The side that is directly over the chip is anti-reflective. Lid dimensions are: Thickness: T=100μm, Width=Length=20mm, Pinhole radius=50μm, Focal Distance: FD=0.6mm.

the azimuth,  $\phi$ , as a function of the illuminated pixels centroid,  $(x, y)$ , and the design parameters shown in Fig. 1:

$$\theta = \arctan \left( \frac{\sqrt{W \cdot (x - x_c)^2 + L \cdot (y - y_c)^2}}{FD} \right) \quad (1)$$

$$\phi = \arctan \left( \frac{L \cdot (y - y_c)}{W \cdot (x - x_c)} \right) \quad (2)$$

Where  $(x_c, y_c)$  is the centroid of the ROI (center of the illuminated region) when  $\theta = 0^\circ$ .  $W=25\mu\text{m}$  and  $L=25\mu\text{m}$  are the pixel width and length, respectively.  $FD=0.6\text{mm}$  is the focal distance, i.e. the distance between the pixel array and the lid.

Fig. 2.(a) displays the system implementation and its optics. The chip is covered with a lid (Fig. 2.(b)) with a radius of  $50\mu\text{m}$ . The lid is anti-reflective on the side that is facing the sensor and reflective on the other side.

For the implementation of this solar sensor, we chose an asynchronous HDR image sensor already reported elsewhere [5], [6]. The sensor has high dynamic range and several operation modes. It was specially intended to operate under high illumination conditions, being specially suitable for the design of a sun sensor that can be exposed to direct sunlight. Its pixels can be configured to pulse with a frequency proportional to the local illumination. Fig. 3 depicts the pixel schematics when it is configured to perform a light to frequency conversion. There is a block that generate pulses with a frequency proportional to illumination. These pulses activate a sequence of asynchronous communication signals to transmit off-chip the coordinates of the pixel that has fired every time that this occurs.

The light-to-frequency conversion block is an astable oscillator. Its operation period is approximately given by:

$$f_{osc} \approx \frac{I_{ph}}{C_{ph} \cdot (V_{DD} - V_{bot})} = \frac{I_{ph}}{C_{ph} \cdot \Delta V} \quad (3)$$

The event rate can be controlled by adjusting the bias voltage  $V_{bot}$ . Pixel transistors have thick gate oxide to allow higher values of  $\Delta V$  and reduce the event flow in conditions of very illumination. Power supply was set to 5V.

### III. EXPERIMENTAL RESULTS

We programmed on the jAER interface [7] a real time algorithm to compute the illuminated pixels centroid and determine the sun position according Equations 1 and 2. Fig. 4 shows the illuminated pixels with the sensor operating.

To calculate the centroid, we apply this simple algorithm periodically:

- 1) We wait until a certain number of events,  $N_{events} \geq 1$ , are received. In the meantime, the coordinates of the pixels that fire  $(x_i, y_j)$  are stored on a memory.
- 2) Once the event number is equal to  $N_{events}$ , we compute the centroid coordinates.

$$x = \frac{1}{N_{events}} \cdot \sum_{i=1}^{N_{events}} x_i, \quad y = \frac{1}{N_{events}} \cdot \sum_{j=1}^{N_{events}} y_j \quad (4)$$

- 3) Once the centroid,  $(x, y)$  is known, the sun position is determined according to Equations 1 and 2.
- 4) The event counter is reset,  $N_{events} = 0$ , and the computation is finished. To calculate the sun position again, go to step #1.

To evaluate the sensor performance, we moved quickly in front of the sensor a light beam modelling the sunlight. The y-coordinate was almost constant while the x-coordinate was changing during the experiment. In Fig. 5, we have plotted the sensor transient response. In Fig. 5.(a) we show the recorded events over time. In Fig. 5.(b), there are the computed angles  $(\theta, \phi)$  for each computed centroid value at time stamps of 5ms. Results are consistent with Equations 1 and 2.

Time-to-first-spike (TFS) operation [8], [9] is possible. To implement it, the centroid position is computed after receiving a programmable number of events,  $N_{events}$ . Then, the sensor is reset and kept idle, enabling the signal  $RES$  in Fig. 3, until the sun position needs to be determined again. In Fig. 6, we display the sensor performance in TFS mode for different number of events. We observe that is possible to determine the sun position, with an acceptable error, after receiving one single event. Results are improved if the number of events is increased. With  $N_{events} = 100$ , angles  $(\theta, \phi)$  computation error is lower than  $0.5^\circ$ .

The event rate is proportional to illumination and the comparators voltage threshold,  $\Delta V$ , in Equation 3. In Fig. 7 the measured event rates for different values of the pixel illuminance, with  $\Delta V = 0.5\text{V}$ , are plotted. There is a trade-off between speed and output data flow. The user can trade off between these parameters depending on illumination levels. The measured pixel event sensitivity is  $S = 0.0762\text{events}/\Delta V \cdot \text{lux}$ , with  $\Delta V = V_{DD} - V_{bot}$ . Under typical application scenarios with direct sunlight, the system employs a few milliseconds to compute the sun position.

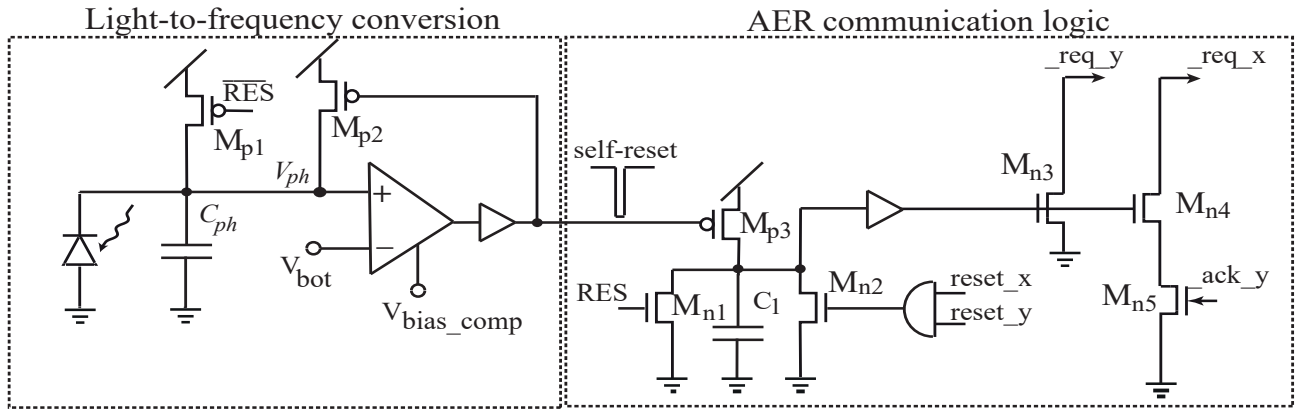


Fig. 3. Pixel schematics. There is circuitry to perform a light to frequency conversion and logic to handle the asynchronous AER communication. Transistor sizes are (W/L,  $\mu\text{m}/\mu\text{m}$ ):  $M_{p1}=1/1$ .  $M_{p2}=3/1$ .  $M_{p3}=0.5/1$ .  $M_{n1}=0.5/0.7$ .  $M_{n2}=0.7/0.7$ .  $M_{n3}=1/0.7$ .  $M_{n4}=M_{n5}=0.5/0.7$ .  $C_{int} = C_1 = 40\text{fF}$ ,  $C_{ph} = 5\text{fF}$ . Bias voltages:  $V_{bot} = 1\text{V}$ ,  $V_{bias\_comp} = 4.3\text{V}$ .

TABLE I  
SYSTEM FEATURES AN STATE-OF-THE-ART COMPARISON.

Work	This Work	Ning et al. [3]	Galileo ESA [4]	Ortega et al. [1]
Type	Event Based Luminance Sensor	APS Digital Sensor	APS Digital Sensor	Analog Sun Sensor
Technology	AMS 0.18 $\mu\text{m}$ HV	0.18 $\mu\text{m}$ 1P4M	UMC 0.18 $\mu\text{m}$	ND
Number of Pixels	128 $\times$ 96	368 $\times$ 368	512 $\times$ 512	2 pairs of photodiodes
Pixel Pitch	25 $\mu\text{m}$ $\times$ 25 $\mu\text{m}$	6.5 $\mu\text{m}$ $\times$ 6.5 $\mu\text{m}$	11 $\mu\text{m}$ $\times$ 11 $\mu\text{m}$	NA
FOV	<b>146<math>^\circ</math></b>	94 $^\circ$	128 $^\circ$	120 $^\circ$
Power Consumption	52mW	42.73mW	520mW	ND
Latency	<b>&lt;5ms@1klux</b>	10frames/s	10frames/s	NA
Dynamic Range	<b>&gt;100dB</b>	52dB	ND	NA
Resolution	0.03 $^\circ$	0.004 $^\circ$	<0.005 $^\circ$	ND
Accuracy	0.0132 $^\circ$ ( $\theta$ ), 0.05 $^\circ$ ( $\phi$ )	0.01 $^\circ$	0.024 $^\circ$	0.15 $^\circ$
Amount of data	<b>1-100 Events</b>	945pixels	1 frame + ROI	4 analog voltages to be readout

Table I compares the sensor features against the art. The amount of data required to compute the sun position is lower than in prior devices based on APS pixels. With only one event, it is possible to achieve competitive results in terms of resolution and accuracy. Latency is much lower. The dynamic range is also higher than the obtained with APS image sensors. The resolution and the accuracy could be improved in further designs by implementing a dedicated pixel for a solar sensor and by refining the optics.

#### IV. CONCLUSIONS

A new sun sensor concept has been presented. It is the very first one that employs a asynchronous pixel matrix whose pixels only send information when they are illuminated. This new approach solves a paradigm traditionally associated to digital sun sensors: pixels that are dark have to be readout. As a result, the output data flow is much more reduced and the operation is faster. The sun position can be resolved with a latency of milliseconds by reading out a reduced number of pixels. In TFS mode, with only the information coming from one single pixel, the sun position can be determined.

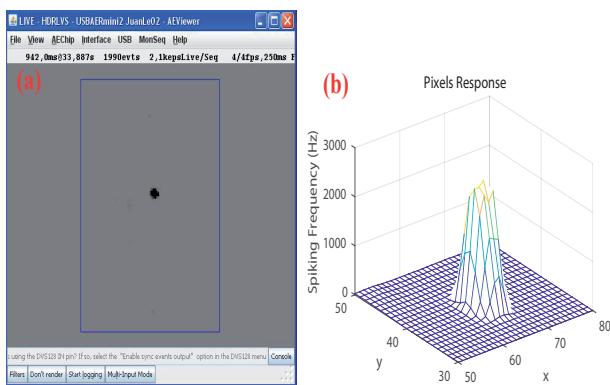


Fig. 4. (a) jAER interface [7] to debug and display the sensor information. The black speckle corresponds to the illuminated region with the sensor operating. (b) Measured spiking frequencies around the illuminated region of interest (ROI).

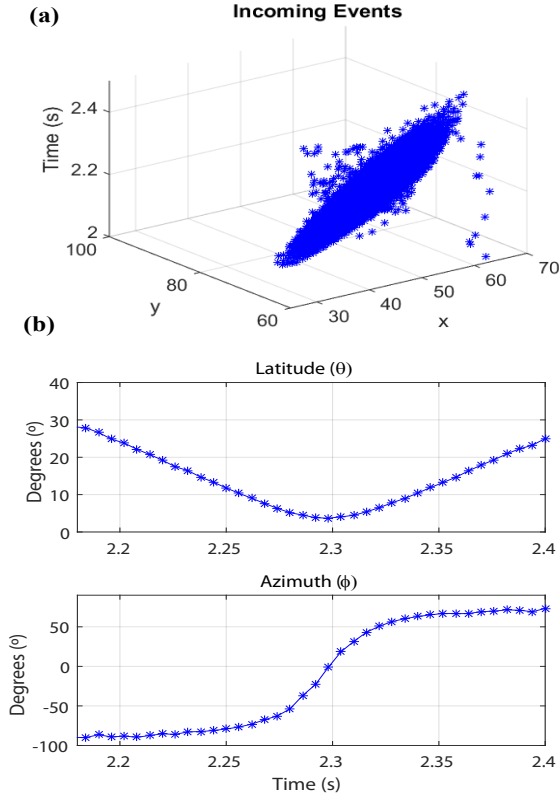


Fig. 5. Sensor's measured transient response. A light beam facing the sensor was rotated to emulate the sun movement. (a) Raster plot: Recorded events versus time. (b) Computed angles ( $\theta, \phi$ ) at time stamps of 5ms indicating the light source position.

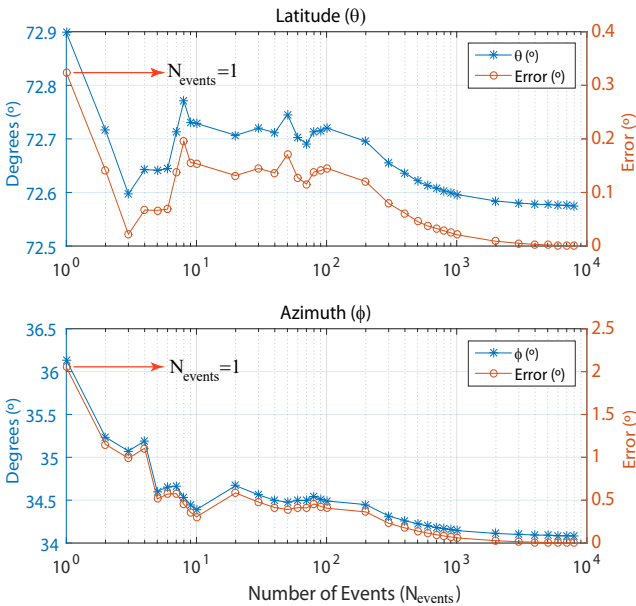


Fig. 6. TFS operation. After resetting the sensor, a certain number of events is received and the sun position is computed. We plot the computed angles ( $\theta, \phi$ ) and the measurement error for different number of incoming events. With only one event, it is possible to gauge the sun position keeping the error low.

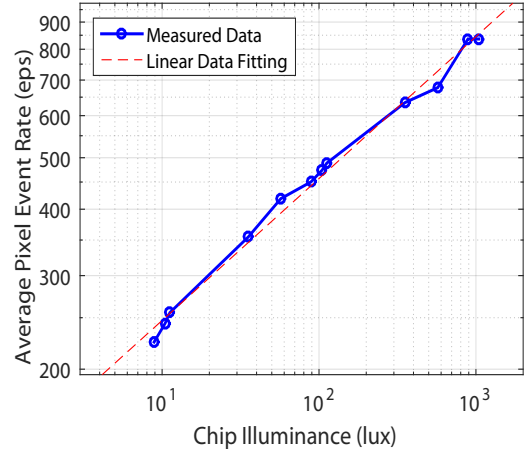


Fig. 7. Blue Trace: measured event rate versus illumination for different chip illuminance values with  $\Delta V = V_{DD} - V_{bot} = 0.5V$ . Red trace: linear data fitting.

## V. ACKNOWLEDGEMENTS

This work was supported in part by the University of Cádiz under Grant PR2016-072; in part by the Spanish Ministry of Economy and Competitiveness under Grant TEC2015-66878-C3-1-R, Co-Funded by ERDF-FEDER; in part by Junta de Andalucía CEICE under Grant TIC 2012-2338 (SMARTCIS-3D); and in part by ONR under Grant N000141410355 (HCELLVIS).

## REFERENCES

- [1] P. Ortega, G. Lopez-Rodriguez, J. Ricart, M. Dominguez, L. M. Castaner, J. M. Quero, C. L. Tarrida, J. Garcia, M. Reina, A. Gras, and M. Angulo, "A miniaturized two axis sun sensor for attitude control of nano-satellites," *IEEE Sensors Journal*, vol. 10, no. 10, pp. 1623–1632, Oct 2010.
- [2] A. Ali and F. Tanveer, "Low-cost design and development of 2-axis digital sun sensor," *Journal of Space Technology*, vol. 1, no. 1, pp. 1–5, Junel 2011.
- [3] N. Xie and A. J. P. Theuwissen, "A miniaturized micro-digital sun sensor by means of low-power low-noise CMOS imager," *IEEE Sensors Journal*, vol. 14, no. 1, pp. 96–103, Jan 2014.
- [4] F. Boldrini, E. Monnini, D. Procopio, B. Alison, W. Ogiers, M. Innocent, A. Pritchard, and S. Airey, "Attitude sensors on a chip: Feasibility study and breadboarding activities," in *Proc. 32nd Annu. AAS Guid. Control Conf.*, February 2009, p. 11971216.
- [5] J. A. Leñero-Bardallo, R. Carmona-Galán, and A. Rodríguez-Vázquez, "A wide linear dynamic range image sensor based on asynchronous selfreset and tagging of saturation events," *IEEE Journal of Solid-State Circuits*, vol. 1, no. 1, pp. 1–13, April 2017.
- [6] —, "A high dynamic range linear vision sensor with event asynchronous and frame-based synchronous operation," in *Electronic Imaging, Image Sensors and Imaging Systems 2016*, February 2016, p. 17.
- [7] "jAER open source project," <http://sourceforge.net/projects/jaer/>.
- [8] M. Barbaro, P. Y. Burgi, A. Mortara, P. Nussbaum, and F. Heitger, "A  $100 \times 100$  pixel silicon retina for gradient extraction with steering filter capabilities and temporal output coding," *IEEE Journal of Solid-State Circuits*, vol. 37, no. 2, pp. 160–172, Feb 2002.
- [9] J. A. Leñero-Bardallo, R. Carmona-Galán, and A. Rodríguez-Vázquez, "A bio-inspired vision sensor with dual operation and readout modes," *Sensors Journal, IEEE*, vol. 16, no. 2, pp. 1–14, January 2016.